ORIGINAL RESEARCH

Effect of gold nanoparticles treatment on the testosterone-induced benign prostatic hyperplasia in rats

Bahaa Al-Trad[1]
Alaa Aljabali[2]
Mazhar Al Zoubi[3]
Malek Shehab[1]
Sahar Omari[1]

[1]Department of Biological Sciences, Yarmouk University, Irbid, Jordan; [2]Department of Pharmaceutical Sciences, Faculty of Pharmacy, Yarmouk University, Irbid, Jordan; [3]Department of Basic Medical Sciences, Faculty of Medicine, Yarmouk University, Irbid, Jordan

Background: Gold nanoparticles (AuNps) are promising agents for prostate cancer therapy. Herein, the in vivo effects of 20 and 50 nm sized AuNps on experimentally induced benign prostatic hyperplasia (BPH) was examined.

Materials and methods: Adult male rats were divided into four groups (n=6–8 each). A negative control group and three groups were injected daily with testosterone (3 mg/kg/ subcutaneously) to induce BPH. Animals receiving testosterone were randomized to untreated BPH group and two BPH groups which were treated intraperitoneally with 20 and 50 nm AuNps (5 mg/kg/daily) in addition to testosterone. After three weeks, histopathological changes and serum levels of testosterone and dihydrotestosterone (DHT) were analyzed. In addition, the prostate tissue levels of transforming growth factor-β_1 (TGF-β_1), vascular endothelial growth factor-a (VEGF-A) and interleukin-6 (IL-6) were measured using ELISA.

Results: There were significant increases in the prostate weight/body weight ratio, serum testosterone and DHT and in the prostate tissue content of TGF-β_1, IL-6 and VEGF-A in the untreated BPH group. histological examination showed morphological abnormalities with more proliferation in the glandular epithelial and stromal area and with abundant epithelial papillary folds in the BPH group. Simultaneous administration of 50 nm AuNps with testosterone tended to increase the prostate weight/body weight ratio and increase the tissue level of IL-6 in compared to the BPH group. Conversely, treatment with 20 nm AuNps significantly reduced the elevated tissue content of TGF-β_1, IL-6, and VEGF-A. Histopathological examination also showed that 20 nm but not the 50 nm AuNps administration ameliorates testosterone-induced prostatic hyperplasia.

Conclusions: In experimentally induced BPH, AuNps can inhibit the progression of BPH in a size-dependent manner. while 20 nm AuNps ameliorate BPH by its inhibitory effects on the prostatic cell proliferation, inflammation and angiogenesis, the 50 nm AuNps could potentially exacerbate the development of BPH in rats, mainly through enhancing the inflammatory process.

Keywords: gold nanoparticles, prostatic hyperplasia, testosterone, rats

Introduction

Benign prostatic hyperplasia (BPH) is defined as out of control growth of the prostate accompanied by lower urinary tract symptoms (LUTS) such as urinary retention and bladder dysfunction.[1] The prevalence of BPH increases with age and it has been found in ~50% of the male population when they are over the age of 40s.[2] BPH can be identified histologically by a progressive nodular increase in the number of epithelial and stromal cells that inflicting the prostate extent expansion and BPH.[1,2]

Correspondence: Bahaa Al-Trad
Departments of Biological Sciences, Yarmouk University, P.O. Box 566, Irbid, 21163 Jordan
Tel +96 277 966 7058
Fax +9 622 721 1117
Email bahaa.tr@yu.edu.jo

Despite the fact that the pathogenesis of BPH is still not well understood yet, numerous lines of evidence suggested that the stimulation of prostatic cellular proliferation with the aid of hormonal and vascular changes appears to be involved in the development and progression of the BPH.[1] The development of BPH can be related to stromal growth due to the activation of mesenchymal-stromal cell proliferation, and epithelial cells overgrowth because of the reduction in the glandular apoptosis.[3,4] Furthermore, chronic inflammation might also play a major role in BPH and prostate cancer improvement.[5,6]

Several growth factors associated with cellular growth, differentiation, apoptosis and epithelial/stromal interaction had been described in the pathophysiology of BPH.[4,7] Transforming growth factor-β_1 (TGF-β_1) is one of the most pro-inflammatory cytokines that play a critical function in the regulation of cells proliferation and cellular apoptosis.[7] Similar to its role in the regulation of the inflammatory process in BPH, it has been shown that the TGF-β_1 level became elevated in BPH samples, which induced stromal and epithelial cells proliferation.[8,9] Increased expression of vascular endothelial growth factor (VEGF), an angiogenic factor, has additionally been observed in BPH.[10]

Currently, the most commonly prescribed medications for the treatment of BPH are the α1-adrenergic receptor antagonists and 5α-reductase inhibitors which improve LUTS associated with BPH by relaxation of smooth muscle in the prostate and the neck of the bladder, and through a reduction in dihydrotestosterone (DHT) production, respectively.[11,12] However, using these drugs are limited because many patients are not able to tolerate their sexual side effects, together with reduced libido and erectile dysfunction.[11,13] Considering this, the search for substances that effectively inhibit the development of BPH and without inducing the side effects associated with the BPH drugs has high priority in biomedical research.

Nanotechnology is a brand-new subject of technology that has a vast range of applications in biology and biomedical fields. Nanomaterials were utilized in numerous biomedical applications for their unique properties, which include their small sizes, biocompatibility and their potential ability to penetrate cellular membrane for carrying drugs.[14,15] Nowadays, gold nanoparticles (AuNPs) are widely used as therapeutic due to their interesting properties from surface reactivity to their low cytotoxicity effect.[15] There are several reports that imply that AuNPs exhibit anti-proliferative,[16,17] anti-angiogenic[18–20] and anti-inflammatory[18,21] activities in a number of disease models, including prostate cancer.[22,23] Since targeting inflammation and angiogenesis processes might be crucial to the development of new therapies to prevent BPH progression, AuNPs may be useful for the treatment of BPH. Therefore, the goal of the present study is to address the effects of 20 nm, and 50 nm sized AuNPs on the histopathological changes related to proliferation, angiogenesis and inflammation in experimentally induced BPH in Sprague-Dawley (SD) rats.

Materials and methods
Fifty nanometer AuNPs synthesis
Fifty nanometer AuNPs synthesis uses a modified sodium citrate approach. In brief, 30 mL of ultra-pure H_2O and 300 μL of a freshly prepared aqueous solution of 1% (w/v) $HAuCl_4$ (Sigma–Aldrich) were added to a 250 mL Erlenmeyer flask (rigorously cleaned with a copious amount of water). The solution was rapidly brought to boil while gently stirring at 150 rpm at ambient temperature. Once the solution reaches boiling (roughly takes around 15 mins), 900 μL of freshly prepared aqueous 1% (w/v) sodium citrate trihydrate (Sigma–Aldrich) solution was added to the reaction mixture. The reaction was left to proceed for 10 mins where the AuNPs formation was completed as indicated by the color transformation to ruby-red. The UV-visible spectrum was used as an indication on the reaction completion.

Twenty nanometer AuNPs synthesis
Similar approach as described previously was adopted to synthesize the ~20 nm AuNPs. In brief, 5 mL of a 1% $HAuCl_4$ aqueous solution was added to a 250 mL Erlenmeyer flask followed by the addition of the $HAuCl_4$ solution, and 4 mL of 0.1 M aqueous solution of K_2CO_3. The volume was adjusted to 100 mL with deionized water. The solution was then mixed well by stirring vigorously (1,000 rpm benchtop vortex) and cooled on ice. With the rapid mixing of the $HAuCl_4$/K_2CO_3, 1 mL of a 7% aqueous sodium ascorbate solution was added, the reaction mixture was maintained in an ice bath for almost 30 mins. The color of the solution at this point turned to a purple-red. This was followed by volume adjustment to 400 mL (total volume) with deionized water, followed by boiling the reaction mixture in a water bath until the color of the suspension turns from purple to red (roughly takes an hour).

Characterization of nanoparticles

Determination of gold content

The concentration of AuNPs was determined spectrophotometrically at ambient room temperature (24–28 ºC) using quartz cuvettes with an optical path length of 1 cm using Beer–Lambert law with an extinction coefficient of 1.8×10^{10} $M^{-1}.cm^{-1}$ for a particle diameter of 50 nm and of 6.3×10^{8} $M^{-1}.cm^{-1}$, respectively as reported in the literature.[24,25]

Surface charge measurement

Zeta potential (ζ) measurements were determined on a Malvern Instruments Zetasizer-Nano ZS. Where 1 mL of 0.2 mg of the generated particles suspended in 0.1 M sodium phosphate buffer pH 7.0. Zeta cells were pre-equilibrated at 21ºC with the buffer. Three independent measurements were recorded each of 12 runs from every batch. The generated data were fitted using the Smoluchowskis approximation assuming Henrys function f(Ka) of 1.5.

Dynamic light scattering (DLS)

DLS measurements were recorded on a DynaPro Titan Wyatt Technology Corporation equipped with a laser wavelength of $\lambda =830$ nm, scattering angle of 2 degrees equipped with Dynamics software version 6.9.2.11. AuNPs suspended in 0.1 M sodium phosphate buffer pH 7.0 at a concentration of $0.5–1$ mg^{-1} cm^{-1} were filtered through 0.1–0.4-micron filters (Millipore) before analysis. The presented data represent four independent measurements every single measurement composed of ten measurements. Data were recorded at ambient room temperature.

Scanning electron microscopy (SEM)

The morphology and the shape of the generated AuNPs were investigated on Quanta FEG SEM, operating at 25 kV in a vacuum with the accelerating voltage set to 1 kV and the working distance was adjusted to 3 mm. The contrast and brightness of the images were adjusted to optimal values, so the AuNPs could be easily distinguished. The length scale with 10–6 nm connected to FEIs MAPS software. Particles were imaged on various magnifications ranging from 1 to 25 k times. Image J version 1.48 was used from 20 particles to determine the shape and the size of dried particles.

Animal studies

All animal experimental procedures were carried out in accordance with the National Institutes of Health guide for the care and use of laboratory animals and approved by the committee of animal ethics at Yarmouk University. Male SD rats aged 3 months and weighing 220–250 g were obtained from animal house/Yarmouk University. After 1 week of acclimation to the laboratory environment, rats were divided into four experimental groups (n=6–8 each). A negative control group received vehicle (corn oil) and three groups were injected daily with testosterone (3 mg/kg/subcutaneously/for three weeks) to induce BPH. Animals receiving testosterone were randomized to untreated BPH group and two BPH groups which were treated intraperitoneally with 20 and 50 nm AuNPs (5 mg/kg/daily) in addition to testosterone. The dose of AuNPs was chosen depending on a pilot study as a dose that not shows any toxicity based on liver and kidney functions parameters with maximal inhibitory effects on the prostate abnormal histological changes (data not shown).

At the end of the experiment, animals were sacrificed under ether anesthesia and their prostates were immediately removed, washed with normal saline solution and divided into two symmetrical parts. The first part was stored in liquid nitrogen, and the second part was fixed in 4% buffered formaldehyde for 4 hrs, and then routinely processed and embedded in paraffin.

Prostate weight/body weight ratio and prostate histology

Serial sections of 5 μm thickness from every set of the experiment were deparaffinized in the dissolving agent (xylene), rehydrated in descendent series of alcohol concentrations and so stained with hematoxylin and eosin. The prostate weight/body weight ratios (PW/BW) of each rat was calculated by dividing prostate weight over body weight (mg/g) and multiplied by 100.

Serum testosterone and DHT levels

Serum testosterone and DHT levels were determined by using testosterone ELISA kit (Biocheck, USA) and DHT ELISA kit (Abnova, USA) following the manufacturer's instructions.

Measurements of TGF-β1, VEGF-A and IL-6 in the prostate

Prostate tissues were homogenized in phosphate buffer saline using a motorized tissue homogenizer (Talboys Engineering Corporation, Montrose, USA). The homogenate was centrifuged for 5 mins at 1,000*g* to remove cell debris and then the supernatant was recentrifuged at 10,000*g* for 10 mins. Commercially available ELISA kits were used according to the manufacturer protocols to identify prostate tissue levels of TGF-β1 (Aviscera Bioscience, USA), VEGF-A (Abcam,

Cambridge, MA) and interleukin-6 (IL-6: Aviscera Bioscience, USA). Protein concentrations were measured by using bicinchoninic acid (BCA) protein assay kit (Sigma, USA) according to the manufacturer's instructions.

Statistical analysis

Statistical analyses of data were performed using the SPSS version 14.0 for Windows (SPSS Inc., Chicago, IL). All data were expressed as means ± SEM. One-way analysis of variance was used to identify the differences between the groups followed by least significant difference post-hoc test analysis. P-value <0.05 was considered a statistically significant difference.

Results

The characterization of the generated AuNPs particles revealed that the generated particles mainly consist of spherical particles (SEM images, Figure 1) with an average hydrodynamic diameter of 51.8±0.7 and 20.2±0.5 nm and with a polydispersity index of 0.26% and 0.19%, respectively, which is consistent with monodisperse and narrow size distribution of the generated AuNPs as shown in Figure 2. Furthermore, the surface zeta potential related to the surface charge of the two sizes of the generated particles was very similar to −40.0±0.2 and −42.2±0.5 mV, respectively (Figure 3). Eliminating any surface charge influence on this study finding and confirming that particles have similar surface properties.

As shown in Table 1 and after three weeks of testosterone and AuNPs treatments, the prostate weight/body weight ratio was significantly higher in the BPH and BPH +20 and

50 nm AuNPs groups in compared to the control rats (P<0.05). However, the prostate weight/body weight ratio tended to be higher in the BPH +50 nm AuNPs group compared to the BPH and BPH +20 nm groups (Table 1; P<0.1). The prostate epithelial thickness was significantly higher in all groups in comparison to the control rats after three weeks of testosterone treatment (Table 1; P<0.05). However, the prostate epithelial thickness was significantly lower in the BPH +20 nm AuNPs group in comparison to the BPH and BPH +50 nm AuNPs groups.

Serum DHT and testosterone levels were increased in the BPH, BPH +20 nm AuNPs and BPH +50 nm AuNPs groups in comparison with the control group (Table 1; P<0.05). Additionally, there were significant increases in the serum DHT and testosterone levels in both the BPH +20 nm AuNPs and BPH +50 nm AuNPs groups compared to the BPH group.

The histological analysis revealed no microscopic anatomical alterations within the prostate gland in the control group as shown in Figure 4. On the other hand, histological microscopic anatomical examination of the prostate in the BPH group showed morphological abnormalities including a higher degree of proliferation in the glandular epithelial and stromal area with focal areas with intraluminal papillary folds and secretion-filled distended ducts. Treatment of the BPH rats with 20 nm but not 50 nm AuNPs ameliorated the above histological abnormalities. Interestingly, dilation of the prostate lumen and an increase in the accumulation of secretory material were observed in the BPH +20 nm AuNPs group, indicating that 20 nm AuNPs enhanced the secretory activity of epithelial cells.
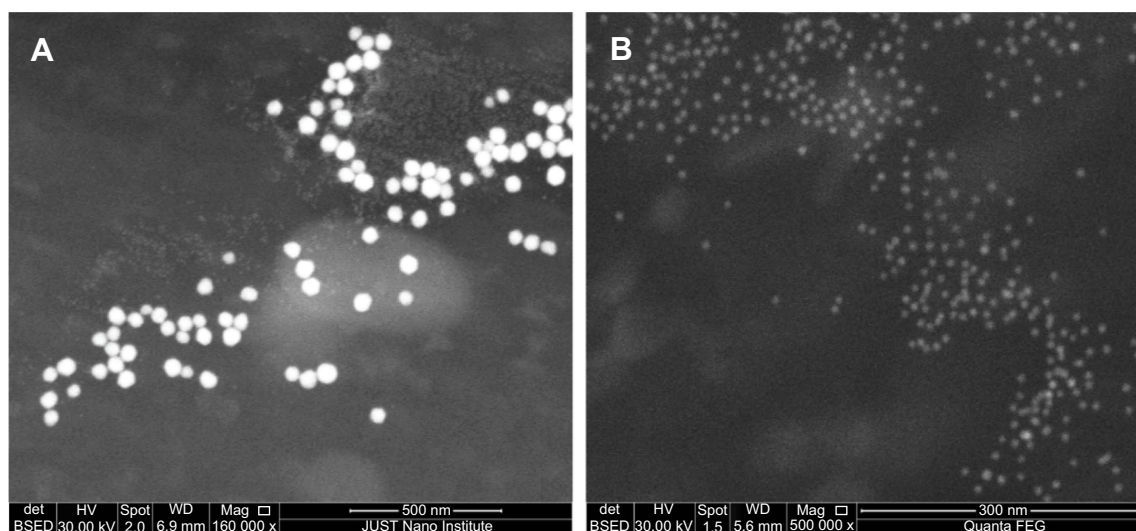

Figure 1 Scanning electron microscopy (SEM) representative images of the generated AuNPs deposited on Si surface. (**A**) 50 nm AuNPs and (**B**) 20 nm AuNPs.
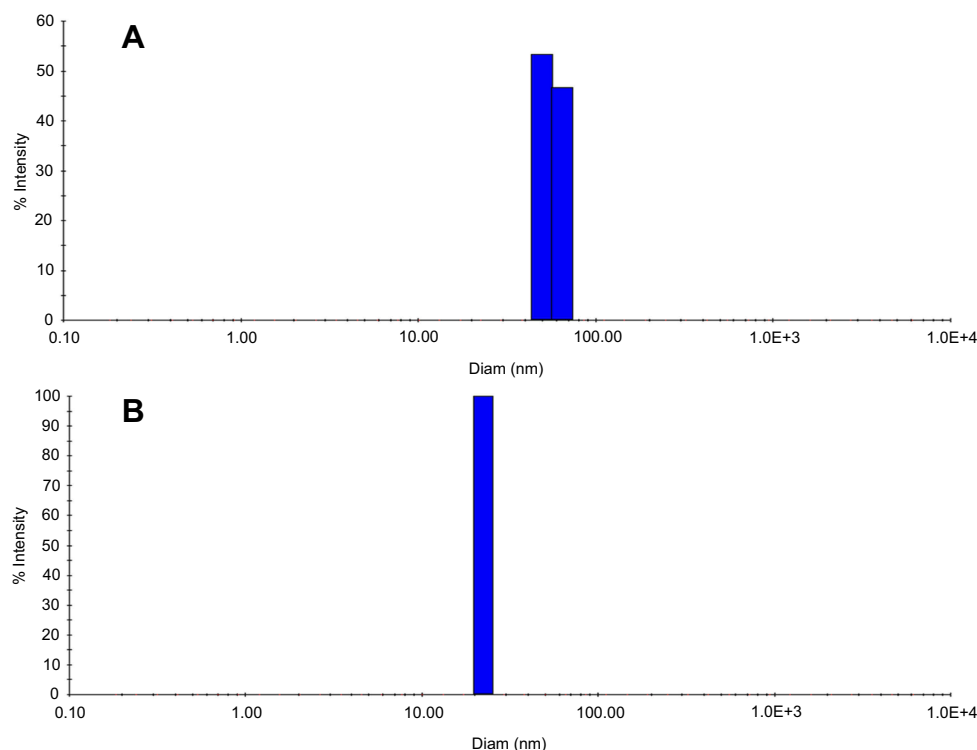
Figure 2 Size distribution of AuNPs as determined by dynamic light scattering (DLS). (**A**) 50 nm AuNPs and (**B**) 20 nm AuNPs. X-axis shows the particles diameter, and the Y-axis represents the nanoparticles size as measured by intensity.
Abbreviations: AuNPs, gold nanoparticles; Diam, diameter.

Moreover, in comparison to the control group, there were significant increases in the prostate tissue content of TGF-β_1 (Figure 5; $P<0.05$), VEGF-A (Figure 6; $P<0.05$) and IL-6 (Figure 7; $P<0.05$) in the untreated BPH group. Simultaneous administration of 20 nm AuNPs and testosterone significantly reduced the elevated tissue content of TGF-β_1, VEGF-A and IL-6. Conversely, treatment with 50 nm AuNPs significantly increased the prostatic tissue level of IL-6 in compared to the BPH group. Fifty nanometer AuNPs were shown to be less effective in blocking the angiogenesis induced by VEGF-A.

Discussion

Considering the anti-inflammatory and the anti-angiogenic properties of AuNPs, as well as their potential to inhibit most cancer cell proliferation, the present study is assessing the in vivo effects of two different sizes of AuNPs on BPH animal model. The main finding of this study is that AuNPs can inhibit the progression of prostatic hyperplasia in a size-dependent manner.

Within the adult prostate, androgens and many polypeptide growth factors are necessary for maintaining the structural and functional integrity of the prostate through controlling of homeostasis between the processes of cell proliferation and cell death (ie, apoptosis).[1] With advancing age, however, over-growth of the prostate happens in humans as BPH because of the imbalance among promoting and inhibiting cell-death signals.[4] It has been suggested that the development of BPH may be associated with both stromal growth, due to active mesenchymal-stromal cell proliferation, and epithelial growth, because of reduced glandular apoptosis.[4,26]

Many growth factors and inflammatory cytokines are associated with epithelial/stromal interaction have been described within the pathogenesis of BPH. It was reported that the level of TGF-β_1, the predominant TGF-β isoform in the prostate, was upregulated in BPH.[8,27] TGF-β has a critical role in the regulation of stromal cell proliferation, differentiation and apoptosis during BPH development.[28] More recent, Hu and his colleagues showed that TGF-β_1 mediated epithelial-mesenchymal transition in BPH-1 cell line.[29] This phenomenon which is one of the theories that have been proposed to explain the pathogenesis of BPH involves the accumulation of mesenchymal-like cells derived from the prostatic epithelium and the endothelium.[30] Unmodified AuNPs reverse the epithelial-mesenchymal transition and downregulate TGF-β1 protein
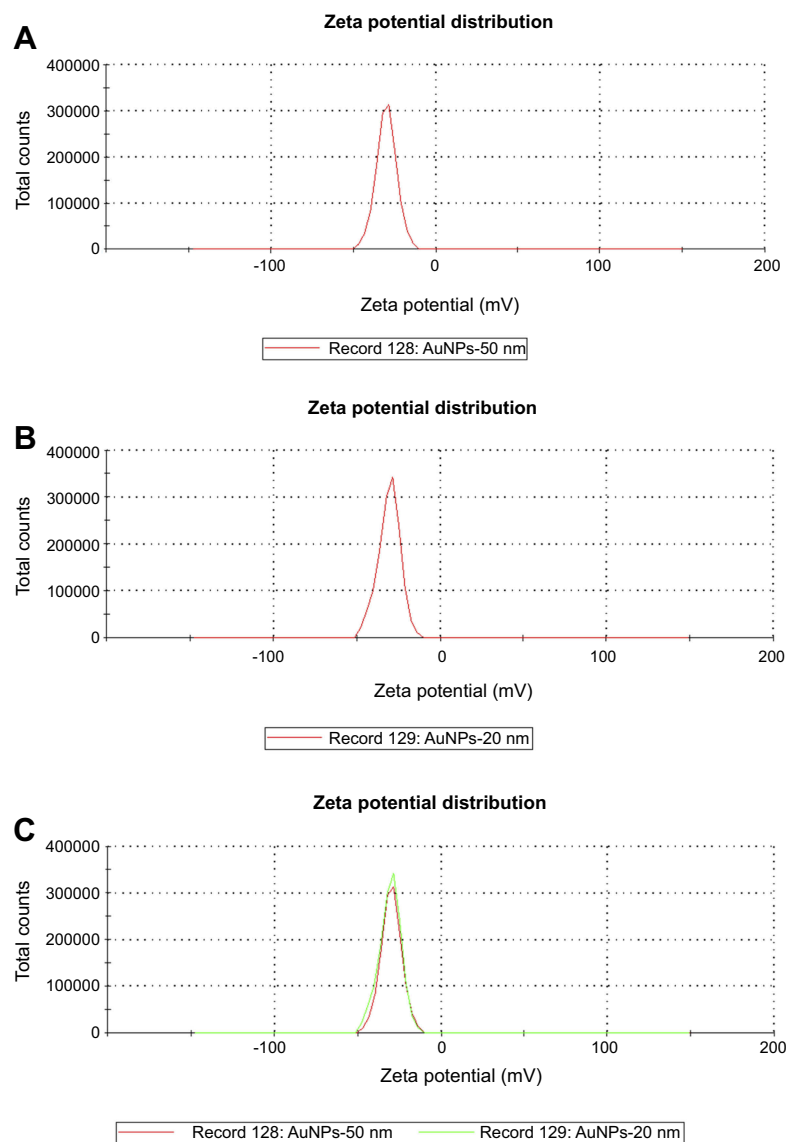
Figure 3 The zeta potential (ζ) distribution of the generated AuNPs.
Abbreviation: AuNPs, gold nanoparticles.

Table I Effects of AuNPs treatment on prostate weight/body weight ratio, prostate epithelial thickness and serum of DHT and testosterone levels

	PW/BW ratio	Epithelial thickness (µm)	Serum DHT (ng/mL)	Serum testoster-one (ng/mL)
Control	0.14±0.01	5.14±0.12	1649.3±52.8	7.30±0.44
BPH	0.28±0.01*	11.53±0.15*	1865.4±25.3*	12.47±0.99*
BPH +20 nm AuNPs	0.27±0.01*	6.95±0.16*	1925.3±21.1$^{#*}$	15.58±0.24$^{*#}$
BPH +50 nm AuNPs	0.34±0.02$^{\$*}$	10.1±0.71*	1933.5±20.1$^{#*}$	15.63±0.32$^{*#}$

Notes: Data represent the mean ± SEM. *$P<0.05$ compared to the control group. $^{#}P<0.05$ compared to the BPH group. $^{\$}P<0.10$ compared to the BPH group.
Abbreviations: AuNPs, gold nanoparticles, DHT, dihydrotestosterone; BPH, benign prostatic hyperplasia; PW/BW, prostate weight/body weight ratio.

in ovarian cancer cells.[17] In the present study, we observed that treatment with 20 nm AuNPs significantly decreased TGF-β_1 levels in the prostate, indicating that the inhibition of TGF-β_1 signaling pathways may play an important role in the inhibitory effect on the progression of prostatic hyperplasia using the 20 nm AuNPs.
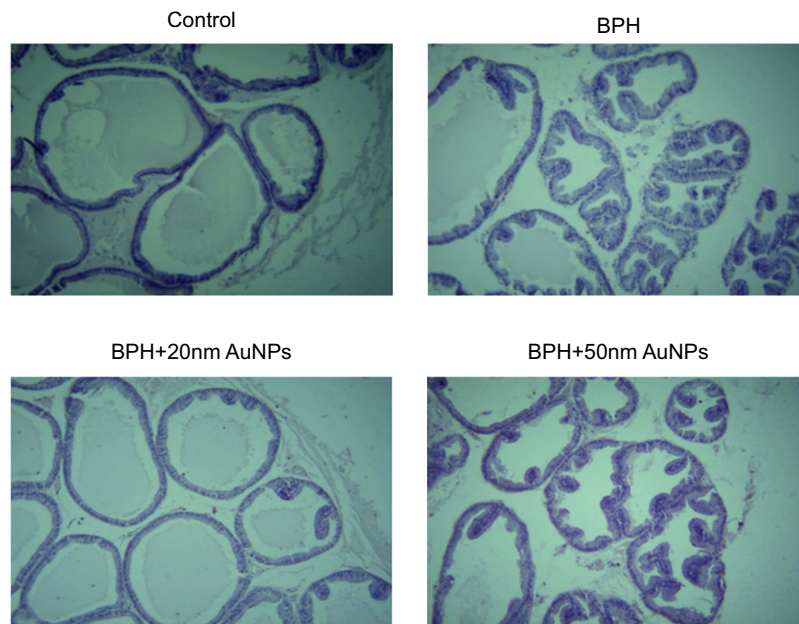
Control

BPH

BPH+20nm AuNPs

BPH+50nm AuNPs

Figure 4 Effect of AuNPs treatment on the histomorphological changes of prostate sections (hematoxylin staining; magnification, ×100). Control group shows no histological alteration in the prostate gland. BPH group exhibit more proliferation in the glandular epithelial and stromal area with several papillary projections into the lumen. BPH +20 nm AuNPsgroup but not BPH +50 nm AuNPs show marked reduction in the epithelial hyperplasia, and the intraluminal papillary folds induced by testosterone.
Abbreviations: BPH, benign prostatic hyperplasia; AuNPs, gold nanoparticles.
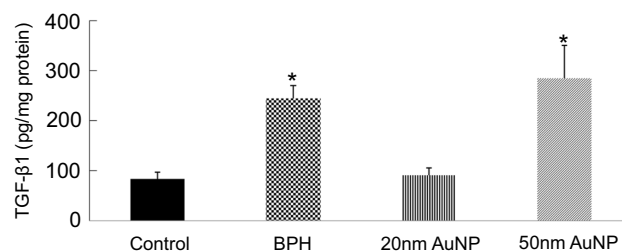
Figure 5 Effect of AuNPs treatment on the prostatic tissue level of TGFβ1. Data represent the mean ± SEM.*$P<0.05$ compared to the control group.
Abbreviations: BPH, benign prostatic hyperplasia; AuNPs, gold nanoparticles; TGF-β1, transforming growth factor-β1.
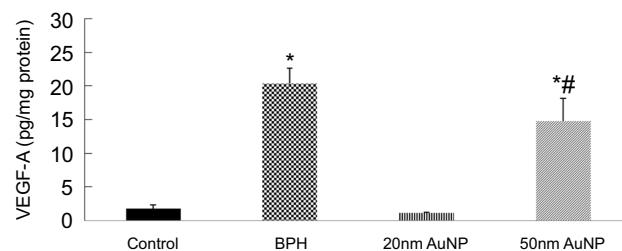

Figure 7 Effect of AuNPs treatment on the prostatic tissue level of IL-6. Data represent the mean ± SEM.*$P<0.05$ compared to the control group. #$P<0.05$ compared to the BPH group.
Abbreviations: BPH, benign prostatic hyperplasia; AuNPs, gold nanoparticles; IL-6, interleukin-6.

Figure 6 Effect of AuNPs treatment on the prostatic tissue level of VEGF-A. Data represent the mean ± SEM.*$P<0.05$ compared to the control group. #$P<0.05$ compared to the BPH group.
Abbreviations: BPH, benign prostatic hyperplasia; AuNPs, gold nanoparticles; VEGF-A, vascular endothelial growth factor-A.

Angiogenesis, which is defined by the formation of new blood vessels from pre-existing vasculature, has been recognized as a key factor in the pathogenesis of
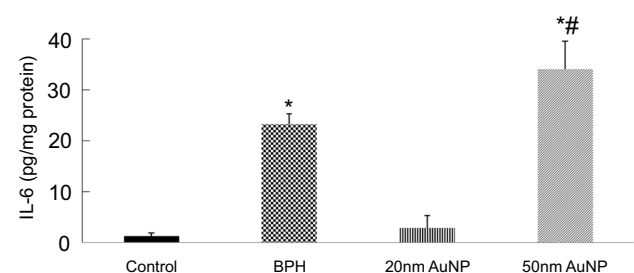
BPH.[10] Given that VEGF is the major driver in the angiogenesis process, increase in the VEGF expression is implicated in the BPH development.[27] Substantial experimental accumulating evidence shows that AuNPs exert anti-angiogenic effects in vitro.[15,16,18,19] AuNPs specifically bound vascular permeability factor/VEGF-165 and basic fibroblast growth factor, two pro-angiogenic heparin-binding growth factors resulting in inhibition of endothelial/fibroblast cell proliferation.[15,19] In the present study, the usefulness of AuNPs as an antiangiogenic is being further confirmed. Our finding as shown in Figure 6 clearly shows that the 20 nm AuNPs inhibits the increase in the prostatic tissue level of VEGF-A in BPH. The current study also showed that the size of AuNPs is

a critical parameter in the mechanism by which AuNPs inhibit angiogenesis. In line with that, 20 nm AuNPs maximally inhibited the VEGF165 induced proliferation of human umbilical vein endothelial cells as compared to 5 and 10 nm AuNPs.[16]

The inflammation role in BPH development was reported in several studies.[5,6] In a large cohort of surgically treated BPH patients, Robert et al, reported that there is a strong association between the inflammatory process and BPH progression.[31] Increased production of pro-inflammatory cytokines such as IL-6, IL-17 and IL-18 has frequently been reported in prostatic tissues of patients with BPH.[5,32] Elevated expression of proinflammatory IL-17 stimulates the production of IL-6 and IL-8, key executors of stromal and epithelial growth in BPH.[1,5,32] Therefore, inflammation is a therapeutic target for BPH. It has been shown that AuNPs downregulated, in a size-dependent manner, the inflammatory process induced by IL-1β dependent pathways in both in vitro and in vivo.[21] A significant down-regulation of abdominal fat tissue TNFα and IL-6 mRNA expression was also observed by the presence of uncoated spherical AuNPs of 21 nm in mice.[33] Our study provides direct evidence that AuNPs treatments can downregulate the prostatic IL-6 level in an experimental animal model of BPH in a size-dependent manner. Besides, the current study showed that IL-6 concentrations in the 20 nm AuNPs + BPH prostate were significantly lower compared to the BPH and 50 nm AuNPs + BPH groups. These findings suggest that the anti-inflammatory effect of 20 nm AuNPs may play a major role in the protective effect of 20 nm AuNPs against BPH. In contrast, AuNPs of 50 nm in size increased the prostatic tissue level of IL-6 significantly compared to the BPH, suggesting that 50 nm AuNPs may induce inflammatory responses that could potentially exacerbate the development of BPH. In the liver and kidney, 50 nm AuNPs caused more severe acute phase expression of proinflammatory cytokines (IL-6 and TNF-α) as compared to smaller sized (10 nm) AuNPs.[34]

We report herein that both 20 and 50 nm sized AuNPs increased serum DHT and testosterone levels. This finding is consistent with the previous report showing that AuNPs treatment elevates blood testosterone levels in male mice without affecting fertility.[35] Moreover, 20 nm but not 50 nm sized AuNPs decreased the epithelial proliferation rate, and this was accompanied by increase in the prostatic secretion activity which might explain the insignificant effect of 20 nm AuNPs on prostate weight/body weight

ratio. In our study, the molecular mechanisms behind this antiproliferative effect were not fully investigated. However, it is clear that the inhibitory effect of 20 nm AuNPs on the progression of prostatic hyperplasia was independent of the circulating DHT. Glucose-capped AuNPs activate cyclin-dependent kinases in human prostate carcinoma cell line DU-145 cells leading to cell cycle acceleration in the G0/G1 phase and the accumulation in the G2/M phase.[22] Additionally, the study by Reznikov et al,[23] demonstrated that AuNPs suppressed human prostate carcinoma cell line DU-145 cells proliferation without causes apoptosis or necrosis. Further studies are still needed to determine the mechanisms of the anti-proliferative effect of AuNPs in both the benign and malignant prostate cells.

Another point worth mentioning is that the variation in the effect of the 20 and 50 nm sized AuNPs in the present study could be attributed to the particle size. Smaller nanoparticle had higher penetration rates in tissues, higher blood concentration post administration and wide biological distribution.[36] In ovarian cancer cells were incubated with 5, 20, 50 and 100 nm AuNPs, the highest intracellular uptake was seen for 5 and 20 nm AuNPs size, and the antiproliferative effect of AuNPs was correlated with their intracellular uptake.[17] Here and by using inductively coupled plasma mass spectrometry; we have found that the 20 nm AuNPs accumulated greater than 50 nm AuNPs in the prostate, as expected (data not shown).

Conclusion

This study is the first to demonstrate that in experimentally induced BPH, AuNPs can inhibit the progression of prostatic hyperplasia in a size-dependent manner. While 20 nm AuNPs ameliorate BPH by its inhibitory effects on the prostatic cell proliferation, inflammation and angiogenesis, the 50 nm AuNPs could potentially exacerbate the development of BPH in rats, mainly through enhancing the inflammatory process.

Acknowledgments

Disclosure

The authors report no conflicts of interest in this work. .

References

1. Briganti A, Capitanio U, Suardi N, et al. Benign prostatic hyperplasia and its aetiologies. *Eur Urol Suppl*. 2009;8(13):865–871. doi:10.1016/j.eursup.2009.11.002

2. Roehrborn CG. Pathology of benign prostatic hyperplasia. *Int J Impot Res*. 2008;20(Suppl 3):S11–S18. doi:10.1038/ijir.2008.55

3. Wang L, Xie L, Tintani F, et al. Aberrant transforming growth factor-beta activation recruits mesenchymal stem cells during prostatic hyperplasia. *Stem Cells Transl Med*. 2017;6(2):394–404. doi:10.5966/sctm.2015-0411

4. Lee KL, Peehl DM. Molecular and cellular pathogenesis of benign prostatic hyperplasia. *J Urol*. 2004;172(5 Pt 1):1784–1791.

5. De Nunzio C, Presicce F, Tubaro A. Inflammatory mediators in the development and progression of benign prostatic hyperplasia. *Nat Rev Urol*. 2016;13(10):613–626. doi:10.1038/nrurol.2016.168

6. Kramer G, Mitteregger D, Marberger M. Is benign prostatic hyperplasia (BPH) an immune inflammatory disease? *Eur Urol*. 2007;51 (5):1202–1216. doi:10.1016/j.eururo.2006.12.011

7. Culig Z, Hobisch A, Cronauer MV, et al. Regulation of prostatic growth and function by peptide growth factors. *Prostate*. 1996;28 (6):392–405. doi:10.1002/(SICI)1097-0045(199606)28:6<392::AID-PROS9>3.0.CO;2-C

8. Kyprianou N, Tu H, Jacobs SC. Apoptotic versus proliferative activities in human benign prostatic hyperplasia. *Hum Pathol*. 1996;27 (7):668–675.

9. Descazeaud A, Weinbreck N, Robert G, et al. Transforming growth factor β-receptor II protein expression in benign prostatic hyperplasia is associated with prostate volume and inflammation. *BJU Int*. 2011;108(2b):E23–E28. doi:10.1111/j.1464-410X.2010.09699.x

10. Sciarra A, Voria G, Mariotti G, Gentile V, Pastore A, Di Silverio F. Histopathological aspects associated with the diagnosis of benign prostatic hyperplasia: clinical implications. *Urol Int*. 2002;69 (4):253–262. doi:10.1159/000066128

11. Bullock TL, Andriole GL Jr. Emerging drug therapies for benign prostatic hyperplasia. *Expert Opin Emerg Drugs*. 2006;11 (1):111–123. doi:10.1517/14728214.11.1.111

12. McVary KT. A review of combination therapy in patients with benign prostatic hyperplasia. *Clin Ther*. 2007;29(3):387–398.

13. Traish AM, Hassani J, Guay AT, Zitzmann M, Hansen ML. Adverse side effects of 5α-reductase inhibitors therapy: persistent diminished libido and erectile dysfunction and depression in a subset of patients. *J Sex Med*. 2011;8(3):872–884. doi:10.1111/j.1743-6109.2010.02157.x

14. Wang EC, Wang AZ. Nanoparticles and their applications in cell and molecular biology. *Integr Biol*. 2014;6(1):9–26. doi:10.1039/c3ib40165k

15. Bhattacharya R, Mukherjee P. Biological properties of "naked" metal nanoparticles. *Adv Drug Deliv Rev*. 2008;60(11):1289–1306. doi:10.1016/j.addr.2008.03.013

16. Arvizo RR, Rana S, Miranda OR, Bhattacharya R, Rotello VM, Mukherjee P. Mechanism of anti-angiogenic property of gold nanoparticles: role of nanoparticle size and surface charge. *Nanomedicine*. 2011;7(5):580–587. doi:10.1016/j.nano.2011.01.011

17. Arvizo RR, Saha S, Wang E, Robertson JD, Bhattacharya R, Mukherjee P. Inhibition of tumor growth and metastasis by a self-therapeutic nanoparticle. *Proc Natl Acad Sci U S A*. 2013;110 (17):6700–6705. doi:10.1073/pnas.1214547110

18. Tsai CY, Shiau AL, Chen SY, et al. Amelioration of collagen-induced arthritis in rats by nanogold. *Arthritis Rheum*. 2007;56(2):544–554. doi:10.1002/art.22401

19. Mukherjee P, Bhattacharya R, Wang P, et al. Antiangiogenic properties of gold nanoparticles. *Clin Cancer Res*. 2005;11(9):3530–3534. doi:10.1158/1078-0432.CCR-04-2482

20. Kalishwaralal K, Sheikpranbabu S, BarathManiKanth S, Haribalaganesh R, Ramkumarpandian S, Gurunathan S. Gold nanoparticles inhibit vascular endothelial growth factor-induced angiogenesis and vascular permeability via Src dependent pathway in retinal endothelial cells. *Angiogenesis*. 2011;14(1):29–45. doi:10.1007/s10456-010-9193-x

21. Sumbayev VV, Yasinska IM, Garcia CP, et al. Gold nanoparticles downregulate interleukin-1β-induced pro-inflammatory responses. *Small*. 2013;9(3):472–477. doi:10.1002/smll.201201528

22. Roa W, Zhang X, Guo L, et al. Gold nanoparticle sensitize radiotherapy of prostate cancer cells by regulation of the cell cycle. *Nanotechnology*. 2009;20(37):375101. doi:10.1088/0957-4484/20/37/375101

23. Reznikov AG, Salivonyk OA, Sotkis AG, Shuba YM. Assessment of gold nanoparticle effect on prostate cancer LNCaP cells. *Exp Oncol*. 2015;37(2):100–104.

24. Aljabali AA, Akkam Y, Al Zoubi MS, et al. Synthesis of gold nanoparticles using leaf extract of ziziphus zizyphus and their anti-microbial activity. *Nanomaterials*. 2018;8(3):174. doi:10.3390/nano8030174

25. Zuber A, Purdey M, Schartner E, et al. Detection of gold nanoparticles with different sizes using absorption and fluorescence based method. *Sens Actuators B Chem*. 2016;227:117–127. doi:10.1016/j.snb.2015.12.044

26. Zhang X, Zhang Q, Zhang Z, Na Y, Guo Y. Apoptosis profiles in benign prostatic hyperplasia: close associations of cell kinetics with percent area density of histologic composition. *Urology*. 2006;68(4):905–910. doi:10.1016/j.urology.2006.05.013

27. Al-Trad B, Al-Zoubi M, Qar J, et al. Inhibitory effect of thymoquinone on testosterone-induced benign prostatic hyperplasia in wistar rats. *Phytother Res*. 2017;31(12):1910–1915. doi:10.1002/ptr.5936

28. Huang X, Lee C. Regulation of stromal proliferation, growth arrest, differentiation and apoptosis in benign prostatic hyperplasia by TGF-beta. *Front Biosci*. 2003;8:s740–s749.

29. Hu S, Yu W, Lv T-J, Chang C-S, Li X, Jin J. Evidence of TGF-β 1 mediated epithelial-mesenchymal transition in immortalized benign prostatic hyperplasia cells. *Mol Membr Biol*. 2014;31(2–3):103–110. doi:10.3109/09687688.2014.894211

30. Alonso-Magdalena P, Brossner C, Reiner A, et al. A role for epithelial-mesenchymal transition in the etiology of benign prostatic hyperplasia. *Proc Natl Acad Sci U S A*. 2009;106(8):2859–2863. doi:10.1073/pnas.0812666106

31. Robert G, Descazeaud A, Nicolaiew N, et al. Inflammation in benign prostatic hyperplasia: a 282 patients' immunohistochemical analysis. *Prostate*. 2009;69(16):1774–1780. doi:10.1002/pros.21027

32. Gandaglia G, Briganti A, Gontero P, et al. The role of chronic prostatic inflammation in the pathogenesis and progression of benign prostatic hyperplasia (BPH). *BJU Int*. 2013;112(4):432–441. doi:10.1111/bju.12118

33. Chen H, Dorrigan A, Saad S, Hare DJ, Cortie MB, Valenzuela SM. In vivo study of spherical gold nanoparticles: inflammatory effects and distribution in mice. *PLoS One*. 2013;8(2):e58208. doi:10.1371/journal.pone.0058208

34. Khan HA, Abdelhalim MA, Alhomida AS, Al-Ayed MS. Effects of naked gold nanoparticles on proinflammatory cytokines mRNA expression in rat liver and kidney. *Biomed Res Int*. 2013;2013:590730. doi:10.1155/2013/590730

35. Li WQ, Wang F, Liu ZM, Wang YC, Wang J, Sun F. Gold nanoparticles elevate plasma testosterone levels in male mice without affecting fertility. *Small*. 2013;9(9-10):1708–1714. doi:10.1002/smll.201201079

36. Hoshyar N, Gray S, Han H, Bao G. The effect of nanoparticle size on in vivo pharmacokinetics and cellular interaction. *Nanomedicine (Lond)*. 2016;11(6):673–692. doi:10.2217/nnm.16.5